Superconducting triangular islands as a platform for manipulating Majorana zero modes

Aidan Winblad[1] and Hua Chen[1, 2]

[1]*Department of Physics, Colorado State University, Fort Collins, CO 80523, USA*
[2]*School of Advanced Materials Discovery, Colorado State University, Fort Collins, CO 80523, USA*

Current proposals on topological quantum computation (TQC) based on Majorana zero modes (MZM) have mostly been focused on coupled-wire architecture which can be challenging to implement experimentally. To explore alternative building blocks of TQC, in this work we study the possibility of obtaining robust MZM at the corners of triangular superconducting islands, which often appear spontaneously in epitaxial growth. We first show that a minimal three-site triangle model of spinless p-wave superconductor allows MZM to appear at different pairs of vertices controlled by a staggered vector potential, which may be realized using coupled quantum dots and can already demonstrate braiding. For systems with less fine-tuned parameters, we suggest an alternative structure of a "hollow" triangle subject to uniform supercurrents or vector potentials, in which MZM generally appear when two of the edges are in a different topological phase from the third. We also discuss the feasibility of constructing the triangles using existing candidate MZM systems and of braiding more MZM in networks of such triangles.

Introduction.—For more than twenty years, Majorana zero modes (MZM) in condensed matter systems have been highly sought after due to their potential for serving as building blocks of topological quantum computation, thanks to their inherent robustness against decoherence and non-Abelian exchange statistics [? ? ? ? ?]. MZM were originally proposed to be found in half-quantum vortices of two-dimensional (2D) topological p-wave superconductors and at the ends of 1D spinless p-wave superconductors [? ?]. Whether a pristine p-wave superconductor [?] has been found is still under debate. However, innovative heterostructures proximate to ordinary s-wave superconductors have been proposed to behave as effective topological superconductors in both 1D and 2D. These include, for example, semiconductor nanowires subject to magnetic fields [? ? ?], ferromagnetic atomic spin chains [? ? ? ? ? ?], 3D topological insulators [? ? ? ?], quantum anomalous Hall insulators [? ? ?], quasi-2D spin-orbit-coupled superconductors with a perpendicular Zeeman field [? ? ? ? ? ?], and planar Josephson junctions [? ? ? ? ? ? ?], etc. It has been a challenging task to decisively confirm the existence of MZM in the various experimental systems due to other competing mechanisms that can potentially result in similar features as MZM do in different probes [? ? ? ? ? ? ? ?]. Other proposals for constructing Kitaev chains through a bottom-up approach, based on, e.g. magnetic tunnel junctions proximate to spin-orbit-coupled superconductors [?], and quantum dots coupled through superconducting links [? ? ?] are therefore promising. In particular, the recent experiment [?] of a designer minimal Kitaev chain based on two quantum dots coupled through tunable crossed Andreev reflections (CAR) offers a compelling route towards MZM platforms based on exactly solvable building blocks.

In parallel with the above efforts of realizing MZM in different materials systems, scalable architectures for quantum logic circuits based on MZM have also been intensely studied over the past decades. A major proposal among these studies is to build networks of T-junctions, which are minimal units for swapping a pair of MZM hosted at different ends of a junction, that allow braiding-based TQC [?]. Alternatively, networks based on coupled wires forming the so-called tetrons and hexons, aiming at measurement-based logic gate operations [?], have also been extensively investigated. To counter the technical challenges of engineering networks with physical wires or atomic chains, various ideas based on effective Kitaev chains, such as quasi-1D systems in thin films [?], cross Josephson junctions [?], scissor cuts on a QAHI [?], and rings of magnetic atoms [?], etc. have been proposed. However, due to the same difficulty of obtaining or identifying genuine MZM in quasi-1D systems mentioned above, it remains unclear how practical these strategies are in the near future.

In this Letter, we propose an alternative structural unit for manipulating MZM, triangular superconducting islands, motivated by the above challenges associated with wire geometries and by the fact that triangular islands routinely appear spontaneously in epitaxial growth [?] on close-packed atomic surfaces. We first show that a minimal "Kitaev triangle" consisting of three sites hosts MZM at different pairs of vertices controlled by Peierls phases on the three edges [Fig. 1 (a)], which can be readily realized using quantum dots. To generalize the minimal model to other means of engineering topologically equivalent triangles, we study the topological phase transitions of quasi-1D ribbons driven by Peierls phases, which can be created by magnetic fields or supercurrents [? ?], and use the resulting phase diagram as a guide to construct finite-size triangles with a hollow interior that host MZM [Fig. 1 (b)]. In the end we discuss possible experimental systems that can realize our proposals and scaled-up networks of triangles for implementing braiding operations of MZM.

Kitaev triangle.—In this section we present an exactly solvable minimal model with three sites forming a "Kitaev triangle" that can host MZM at different pairs of
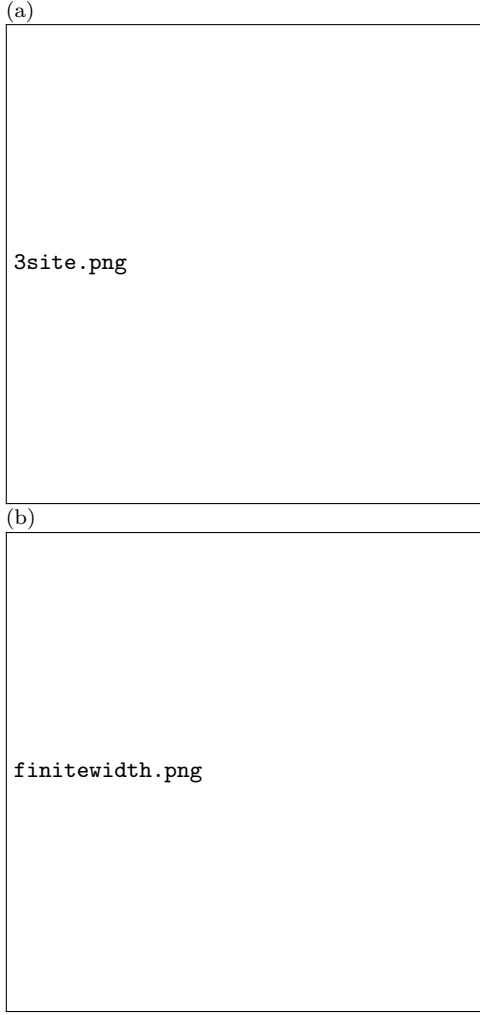
(a)

(b)

FIG. 1. Schematics of two triangle structures proposed in this work. (a) Three-site Kitaev triangle with bond-dependent Peierls phases. (b) Hollow triangular island with a uniform vector potential.

vertices controlled by Peierls phases on the edges. The Bogoliubov-de Gennes (BdG) Hamiltonian includes complex hopping and p-wave pairing between three spinless fermions forming an equilateral triangle [Fig. 1 (a)]:

$$\mathcal{H} = \sum_{\langle jl \rangle} (-te^{i\phi_{jl}} c_j^\dagger c_l + \Delta e^{i\theta_{jl}} c_j c_l + \text{h.c.}) - \sum_j \mu c_j^\dagger c_j, \quad (1)$$

where t is the hopping amplitude, Δ is the amplitude of the (2D) p-wave pairing, μ is the chemical potential, θ_{jl} is the polar angle of $\mathbf{r}_{jl} = \mathbf{r}_l - \mathbf{r}_j$ (the x axis is chosen to be along $\mathbf{r}_{12}$), consistent with $\{c_l^\dagger, c_j^\dagger\} = 0$. ϕ_{jl} is the Peierls phase due to a bond-dependent vector potential $\mathbf{A}$ to be specified below (the nearest neighbor distance a is chosen to be the length unit hereinbelow):

$$\phi_{jl} = \frac{e}{\hbar} \int_{\mathbf{r}_j}^{\mathbf{r}_l} \mathbf{A} \cdot d\mathbf{l} = -\phi_{lj} \quad (2)$$

where $e > 0$ is the absolute value of the electron charge.

Below we use the natural units $e = \hbar = 1$. To get the conditions for having MZM in this model we rewrite $\mathcal{H}$ in the Majorana fermion basis $a_j = c_j + c_j^\dagger$, $b_j = \frac{1}{i}(c_j - c_j^\dagger)$ [?]:

$$\mathcal{H} = -\frac{i}{2} \sum_{\langle jl \rangle} \Big[(t \sin \phi_{jl} - \Delta \sin \theta_{jl}) \, a_j a_l \quad (3)$$

$$+ (t \sin \phi_{jl} + \Delta \sin \theta_{jl}) \, b_j b_l$$

$$+ (t \cos \phi_{jl} - \Delta \cos \theta_{jl}) \, a_j b_l$$

$$- (t \cos \phi_{jl} + \Delta \cos \theta_{jl}) \, b_j a_l \Big] - \frac{i\mu}{2} \sum_j a_j b_j$$

For concreteness we consider the Kitaev limit $t = \Delta$, $\mu = 0$, and choose $\phi_{12} = 0$ so that sites 1 and 2 alone form a minimal Kitaev chain with $\mathcal{H}_{12} = itb_1 a_2$ and hosting MZM a_1 and b_2. In order for the MZM to persist in the presence of site 3, one can choose ϕ_{23} and ϕ_{31} so that all terms involve these Majorana operators cancel out. For example, consider the $2-3$ bond, for which $\theta_{23} = 2\pi/3$, we require

$$\sin \phi_{23} + \sin \frac{2\pi}{3} = \cos \phi_{23} + \cos \frac{2\pi}{3} = 0 \quad (4)$$

which means $\phi_{23} = -\pi/3$. Similarly one can find $\phi_{31} = -\phi_{13} = -\pi/3$. The three Peierls phases can be realized by the following staggered vector potential

$$\mathbf{A} = [1 - 2\Theta(x)] \frac{2\pi}{3\sqrt{3}} \hat{\mathbf{y}} \quad (5)$$

where $\Theta(x)$ is the Heavisde step function. In fact, using a uniform $\mathbf{A} = \frac{2\pi}{3\sqrt{3}} \hat{\mathbf{y}}$, which corresponds to $\phi_{23} = -\pi/3 = -\phi_{31}$ also works, since the existence of a_1 is unaffected by ϕ_{23}. However, in this case the counterpart of b_2 is not localized on a single site. For the same reason, the above condition for MZM localized at triangle corners can be generalized to Kitaev chains forming a triangular loop, as well as to finite-size triangles of 2D spinless p-wave superconductors in the Kitaev limit, as the existence of a_1 and b_2 are only dictated by the vector potential near the corresponding corners. It should be noted that in the latter case, 1D Majorana edge states will arise when the triangle becomes larger, and effectively diminishes the gap that protects the corner MZM. On the other hand, for the longer Kitaev chain, due to the potential practical difficulty of controlling further-neighbor hopping and pairing amplitudes, it is better to resort to the approach of controlling the individual topological phases of the three edges which will be detailed in the next section.

We next show that the minimal Kitaev triangle suffices to demonstrate braiding of MZM. To this end we consider a closed parameter path linearly interpolating between

the following sets of values of ϕ_{jl}:

$$(\phi_{12}, \phi_{23}, \phi_{31}) = \left(0, -\frac{\pi}{3}, -\frac{\pi}{3}\right) \equiv \boldsymbol{\phi}_1 \qquad (6)$$

$$\rightarrow \left(-\frac{\pi}{3}, -\frac{\pi}{3}, 0\right) \equiv \boldsymbol{\phi}_2$$

$$\rightarrow \left(-\frac{\pi}{3}, 0, -\frac{\pi}{3}\right) \equiv \boldsymbol{\phi}_3$$

$$\rightarrow \boldsymbol{\phi}_1$$

It is straightforward to show that at $\boldsymbol{\phi}_2$ and $\boldsymbol{\phi}_3$ there are MZM located at sites $3, 1$ and $2, 3$, respectively. Therefore the two original MZM at sites $1, 2$ should switch their positions at the end of the adiabatic evolution.
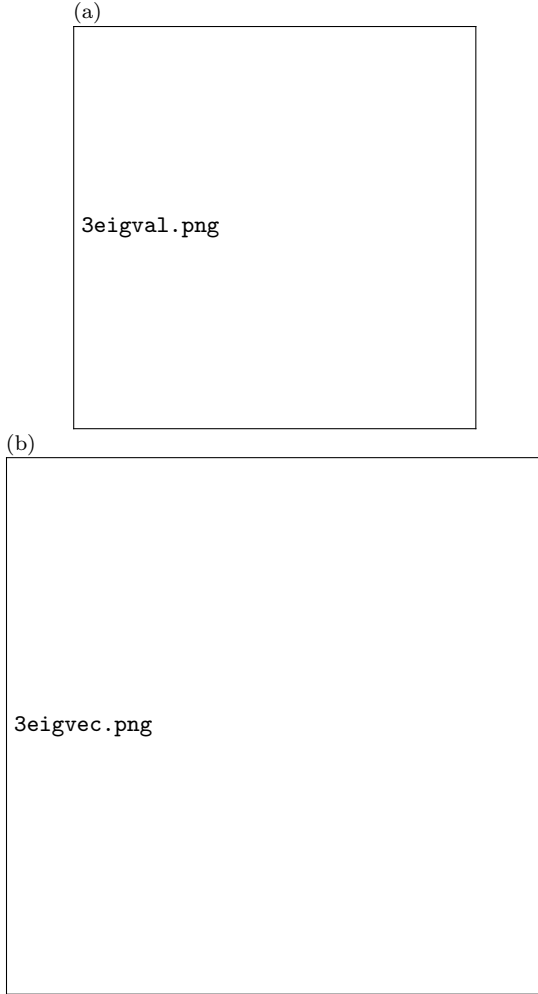
(a)

(b)

FIG. 2. (a) Evolution of the eigenvalues of the 3-site Kitaev triangle along the closed parameter path for ϕ on the three edges. (b) MZM wavefunctions at different points of the parameter path. Clockwise from the upper left panel: $\boldsymbol{\phi}_1 \rightarrow \frac{1}{2}(\boldsymbol{\phi}_1 + \boldsymbol{\phi}_2) \rightarrow \boldsymbol{\phi}_2 \rightarrow \boldsymbol{\phi}_3$.

Indeed, Fig. 2 shows that the MZM stays at zero energy throughout the parameter path that interchanges their positions. To show that such an operation indeed

realizes braiding, we explicitly calculated the many-body Berry phase of the evolution [? ? ?] and found the two degenerate many-body ground states acquire a $\frac{\pi}{2}$ difference in their Berry phases as expected [?]. **Add a section on details of the Berry phase calculation in Supplementary Material.** Compared to the minimum T-junction model with four sites [?], our Kitaev triangle model only requires three sites to achieve braiding between two MZM, and is potentially also easier to engineer experimentally. In the next section we will show that a more mesoscopic hollow-triangle structure can achieve similar results and may be preferred in other materials platforms.

Hollow triangles.—For systems with less fine-tuned Hamiltonians than the minimal model in the previous section, it is more instructive to search for MZM based on topological arguments. In this section we show that MZM generally appear at the corners of a hollow triangle, which can be approximated by joining three finite-width chains or ribbons whose bulk topology is individually tuned by the same uniform vector potential.

To this end, we first show that topological phase transitions can be induced by a vector potential in a spinless p-wave superconductor ribbon. In comparison with similar previous proposals that mostly focused on vector potentials or supercurrents flowing along the chain [? ?], we consider in particular the tunability by varying the direction of the vector potential relative to the length direction of the ribbon, which will become instrumental in a triangular structure.

Consider Eq. (1) on a triangular lattice defined by unit-length lattice vectors $(\mathbf{a}_1, \mathbf{a}_2) = (\hat{\mathbf{x}}, \frac{1}{2}\hat{\mathbf{x}} + \frac{\sqrt{3}}{2}\hat{\mathbf{y}})$ with W unit cells along $\mathbf{a}_2$ but infinite unit cells along $\mathbf{a}_1$, and assume the Peierls phases are due to a uniform vector potential $\mathbf{A}$ so that $\phi_{jl} = \mathbf{A} \cdot \mathbf{r}_{jl}$. We also introduce $\mathbf{a}_3 \equiv -\mathbf{a}_1 + \mathbf{a}_2$ for later convenience. The Hamiltonian is periodic along x and can be Fourier transformed through $c_{m,n}^\dagger = \frac{1}{\sqrt{N}}\sum_k c_{k,n}^\dagger e^{-ikm}$, where m, n label the lattice sites as $\mathbf{r}_{m,n} = m\mathbf{a}_1 + n\mathbf{a}_2$. The resulting momentum space Hamiltonian can be written as the following block form up to a constant

$$\mathcal{H} = \frac{1}{2}\sum_k \Psi_k^\dagger \begin{pmatrix} h_t(k) & h_\Delta(k) \\ h_\Delta^\dagger(k) & -h_t^*(-k) \end{pmatrix} \Psi_k \qquad (7)$$

$$\equiv \frac{1}{2}\sum_k \Psi_k^\dagger H(k)\Psi_k$$

where $\Psi_k \equiv (c_{k,1}, \ldots, c_{k,W}, c_{-k,1}^\dagger, \ldots c_{-k,W}^\dagger)^T$. $h_t(k)$ is a $W \times W$ Hermitian tridiagonal matrix with $(h_t)_{n,n} = -2t\cos(k + \mathbf{A} \cdot \mathbf{a}_1) - \mu$ and $(h_t)_{n,n+1} = -t\left(e^{i(-k+\mathbf{A}\cdot\mathbf{a}_3)} + e^{i\mathbf{A}\cdot\mathbf{a}_2}\right)$. $h_\Delta(k)$ is a $W \times W$ tridiagonal matrix with $(h_\Delta)_{n,n} = -2i\Delta\sin k$ and $(h_\Delta)_{n,n\pm1} = \mp\Delta\left[e^{-i(\pm k+\frac{2\pi}{3})} + e^{-i\frac{\pi}{3}}\right]$.

By transforming Eq. (7) to the Majorana basis using

the unitary transformation:

$$U \equiv \frac{1}{\sqrt{2}} \begin{pmatrix} 1 & 1 \\ -i & i \end{pmatrix} \otimes \mathbb{I} \qquad (8)$$

where $\mathbb{I}$ is a $W \times W$ identity matrix, and defining $A_k \equiv -iUH(k)U^\dagger$, not to be confused with the vector potential, one can calculate the Majorana number [?] $\mathcal{M}$ of the 1D ribbon as [?]

$$\mathcal{M} = \text{sgn}\left[\text{Pf}(A_{k=0})\text{Pf}(A_{k=\pi})\right] \qquad (9)$$

where Pf stands for the Pfaffian of a skew-symmetric matrix [?]. When $\mathcal{M} = -1$, the 1D system is in a nontrivial topological phase with MZM appearing at open ends of semi-infinite ribbons, and otherwise for $\mathcal{M} = 1$.
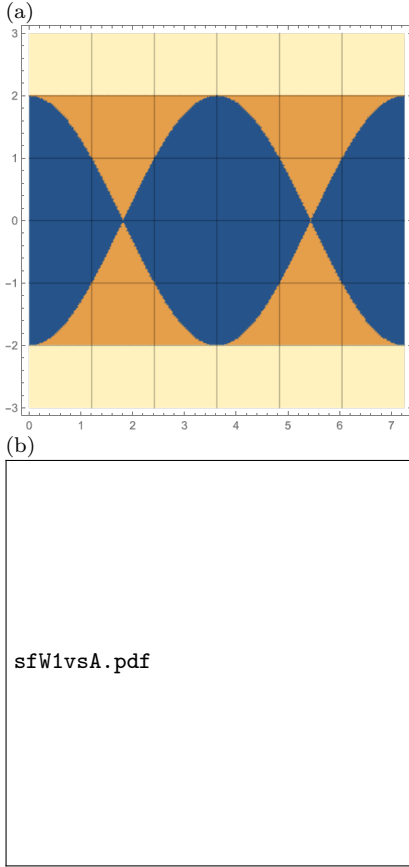

(a)

(b)

sfW1vsA.pdf

FIG. 3. (a) Topological phase diagram for a $W = 1$ triangular chain with the Hamiltonian Eq. (7) obtained by overlapping the $\mathcal{M}(A, \mu)$ plots of 1D chains with $\mathbf{A} = A\hat{\mathbf{y}}$ and $\mathbf{A} = A(\frac{\sqrt{3}}{2}\hat{\mathbf{x}} + \frac{1}{2}\hat{\mathbf{y}})$. (**Color scheme: XXX**–$\mathcal{M} = 1$, **XXX**–$\mathcal{M} = -1$, **XXX**–$\mathcal{M} = 0$) (b) Near-gap BdG eigen-energies vs A for a finite triangle with edge length $L = 50$, $W = 1$, and $\mu = 1.6$.

In Fig. 3 (a) we show the topological phase diagrams for a 1D ribbon with width $W = 1$, $\mathbf{A} = A\hat{\mathbf{y}}$ and $\mathbf{A} = A(\frac{\sqrt{3}}{2}\hat{\mathbf{x}} + \frac{1}{2}\hat{\mathbf{y}})$ superimposed (see below). We found

that the vector potential component normal to the ribbon length direction has no effect on the Majorana number, nor does the sign of its component along the ribbon length direction. However, topological phase transitions can be induced by varying the size of the vector potential component along the ribbon, consistent with previous results [? ?]. These properties motivate us to consider the structure of a hollow triangle formed by three finite-width ribbons subject to a uniform vector potential $\mathbf{A} = A\hat{\mathbf{y}}$ as illustrated in Fig. 1 (b). The XXX color on the phase diagram Fig. 3 (a) therefore means that where the bottom edge and the two upper edges of the hollow triangle have different $\mathcal{M}$, which should give rise to MZM localized at the two bottom corners if the triangle is large enough so that bulk-edge correspondence holds, and gap closing does not occur at other places along its edges.

To show that corner MZM indeed appear when the conditions given by the phase diagram Fig. 3 (a) are met, we directly diagonalize the BdG Hamiltonian of a finite hollow triangle with edge length $L = 50$ and width $W = 1$. Fig. 3 (b) shows the spectral flow (BdG eigen-energies evolving with increasing vector potential A) close to zero energy at chemical potential $\mu = 1.6$. Indeed, zero-energy modes appear in the regions of μ and A consistent with the phase diagram (except when the bulk band gap is too small [?] This is referring to some less ideal parameters and the larger W cases.). Hollow triangles with larger larger W also have qualitatively similar behavior, although the phase diagrams are more complex [?]. The eigenfunctions for the zero-energy modes at $A = XXX$ and $\mu = 1.6$ in Fig. 4 (b) also confirm their spatial localization at the bottom corners of the triangle.

We finally show that rotating the uniform vector potential in-plane can manipulate the positions of the MZM without hybridizing them with bulk states for certain ranges of μ and A. Fig. 4 (a) plots the spectral flow versus the in-plane azimuthal angle of $\mathbf{A}$, which clearly shows that the zero-energy modes persist throughout the rotation and the bulk gap never closes. Figs. 4 (b-d) plot the BdG wavefunctions of the MZM at special values of φ. One can see that the two MZM seem to cycle through the three vertices by following the rotation of $\boldsymbol{A}$. The robustness of the MZM therefore requires the condition of two edges being in a different topological phase from the third one to be satisfied throughout the rotation. Such a criterion combined with the individual phase diagrams of the edges can help isolate the desired parameter regions of μ and A. We also note that the positions of the MZM do not interchange after φ increases from 0 to π, different from the situation of the minimal Kitaev triangle in Fig. 2. The reason is that the MZM in the latter case are not due to bulk-boundary correspondence [the values of $A = \frac{2\pi}{3\sqrt{3}}$ and $\mu = 0$ are a critical point in the phase diagram Fig. 3 (a)]. While the positions of the MZM at special points along the parameter path in the hollow triangle case have to be additionally constrained by the bulk topological phases of the three edges, that for the Kitaev triangle have more flexibility and are also
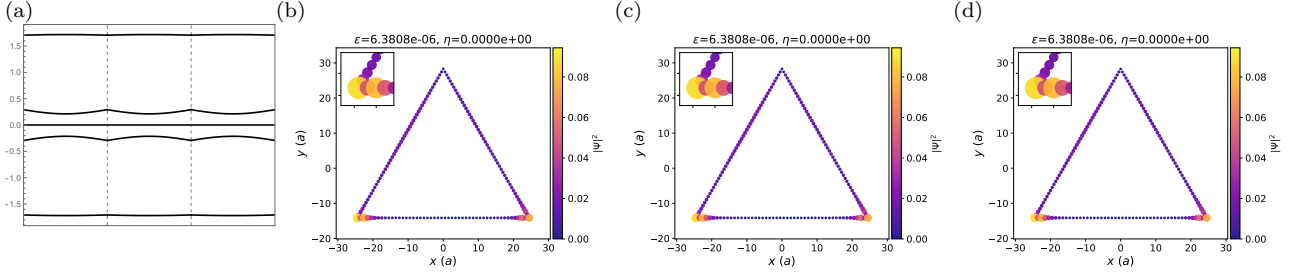
FIG. 4. (a) Spectral flow of a hollow triangle with $W = 1$, $L = 50$, $\mu = 1.6$, and $A = XXX$ with increasing rotation angle φ, defined through $\mathbf{A} = A(\cos\varphi\hat{\mathbf{x}} + \sin\varphi\hat{\mathbf{y}})$. (b-d) BdG eigenfunction $|\Psi|^2$ summed over the two zero modes at $\varphi = 0, \frac{\pi}{6}$, and $\frac{\pi}{3}$, respectively.

protected by the finite size of the system.

Discussion.—The hollow interior of the triangles considered in this work is needed for two reasons: (1) $W \ll L$ is required for bulk-edge correspondence based on 1D topology to hold; (2) A finite W is needed to gap out the chiral edge states of a 2D spinless p-wave superconductor based on which Eq. (7) is written. The latter is not essential if one does not start with a spinless p-wave supercondutor but a more realistic model such as the Rashba+Zeeman+s-wave pairing model. On the other hand, the former constraint may also be removed if one uses the Kitaev triangle. Nonetheless, an effective 3-site Kitaev triangle may emerge as the effective theory of triangular structures if a three-orbital low-energy Wannier basis can be isolated, similar to the continuum theory of Moire structures. We also note in passing that the corner MZM in our triangles appear due to different reasons from that in higher-order topological superconductors [REF].

For possible physical realizations of our triangles, immediate choices are quantum dots forming a Kitaev triangle [**?**], Planar Josephson junctions or cuts on QAHI/superconductor heterostructures [**?**] that form a hollow triangle, and triangular atomic chains assembled by an STM tip [**?**] on a close-packed surface. The quantum-dot platform may be advantageous in the convenience of implementing parity readout by turning the third vertex temporarily into a normal quantum dot [**? ? ?**]. Looking into the future, it is more intriguing to utilize the spontaneously formed triangular islands in epitaxial growth [**?**] with the center region removed either physically by lithography/ablation, or electrically by gating. To create a staggered vector potential or supercurrent profile for the Kitaev triangle, one can use a uniform magnetic field, corresponding to a constant vector potential gradient, plus a uniform supercurrent that controls the position of the zero. It is also possible to use two parallel superconducting wires with counter-propagating supercurrents proximate to the triangle.

A tentative design for braiding more than two MZM based on our triangles is schematically illustrated in Fig. 5. The neighboring triangles share vertices through gated gap regions so that MZM pairs can be created at dif-
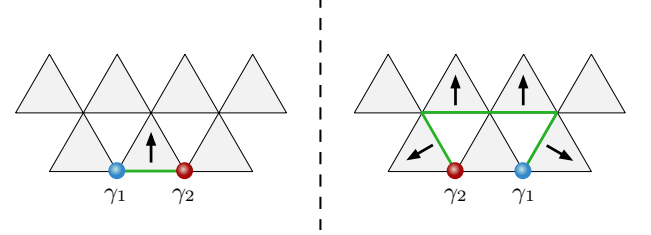

FIG. 5. Network of tunable topological superconducting hollow triangular islands. The left panel shows the initialization of two MZMs γ_1 and γ_2. The right panel depicts the MZMs after a braiding operation. The arrows depict which island has an inhomogeneous vector potential applied and in general direction for a step-function. Green lines shows which edges are topologically nontrivial. Think of a process for braiding two of four MZM.

ferent vertices in individual triangles, while shuffled and transported through different triangles by controlling the gates at shared vertices, that fuse MZM but do not create additional gap closing events.

Our work provides a versatile platform for manipulating MZM based on currently available candidate MZM systems and can be more advantageous than the coupled wire geometry in demonstrating the non-Abelian nature of MZM in near term devices.